IAU Symposium 210: MODELLING OF STELLAR ATMOSPHERES,
Uppsala, Sweden, 17 - 21 June 2002

Acoustic waves in the solar chromosphere - Numerical simulations with COBOLD

Sven Wedemeyer[1], **Bernd Freytag**[2], **Matthias Steffen**[3], **Hans-Günter Ludwig**[4], **Hartmut Holweger**[1]

[1] Institut für Theoretische Physik und Astrophysik, Universität Kiel, Germany
[2] Astronomical Observatory, University of Uppsala, Sweden
[3] Astrophysikalisches Institut Potsdam, Germany
[4] Lund Observatory, Lund, Sweden

e-mail: wedemeyer@astrophysik.uni-kiel.de

Introduction

It is generally assumed that the motions at the top of the solar convection zone generate **acoustic waves** which propagate upwards towards higher layers. Dissipation of these acoustic waves at chromospheric heights might provide a sufficient amount of energy to account for the observed chromospheric emission.
Our aim is to check this **heating mechanism** with detailed numerical simulations. With **COBOLD**, a radiation hydrodynamics code developed by B. Freytag and M. Steffen, we are able to compute 2-D and 3-D models which include the upper convection zone, the photosphere and the **chromosphere**, thus describing the generation, propagation, and dissipation of acoustic waves in a self-consistent way in the same model.

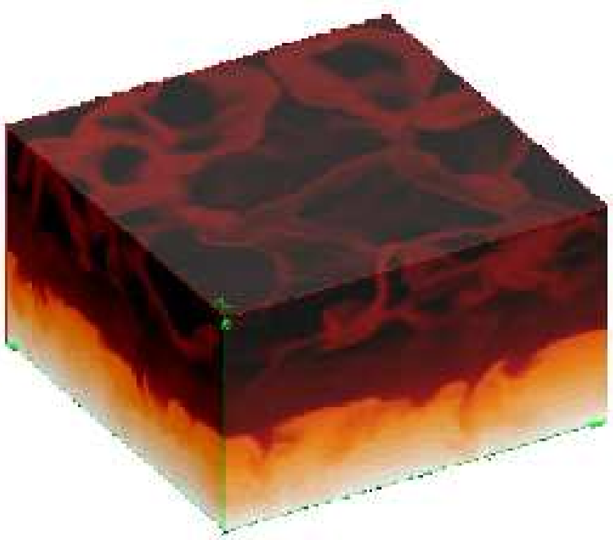

Fig.1: Illustration of a 3-D model, extending from the top of the convection zone to the low/middle chromosphere (internal energy).

Numerical Simulations with COBOLD

COBOLD allows the time-dependent solution of the hydrodynamic equations (conservation of mass, momentum, and energy) and radiative transfer for a fully compressible, chemically homogeneous plasma in 2-D and 3-D. Magnetic fields are not included, restricting this version of COBOLD to internetwork regions.
Cartesian grid: Our actual models consist horizontally (x, y) of 140 grid points with a constant resolution of 40 km, leading to an extension of 5600 km (∼7".7). The 200 vertical (z) grid points are non-equidistant with a resolution of 46 km at the bottom (-1300 km below $\tau_{5000} \approx 1$) which decreases with height down to 12 km for the photosphere and chromosphere. The models include the chromosphere up to a height of $\sim$ 1800 km above $\tau_{5000} \approx 1$, thus leading to a total vertical extension of $\sim$ 3100 km (Fig.1).
Opacity: For the 3-D model which is presented here we used a Rosseland mean opacity table based on data of **OPAL** (Iglesias et al., 1992) and **PHOENIX** (Hauschildt et al.,1997). (The latter includes contributions from molecules.) Additionally, a Rosseland mean and a frequency-dependent table (multi-group) are available for **ATLAS6** opacities (Kurucz, 1970).
Boundary conditions: We use periodic boundaries for the sides of the models and an open lower boundary with entropy and pressure adjustment. The upper boundary is transmitting. There the temperature of the inflowing material is altered towards an temperature $T_{\rm top}$ on a characteristic time scale.

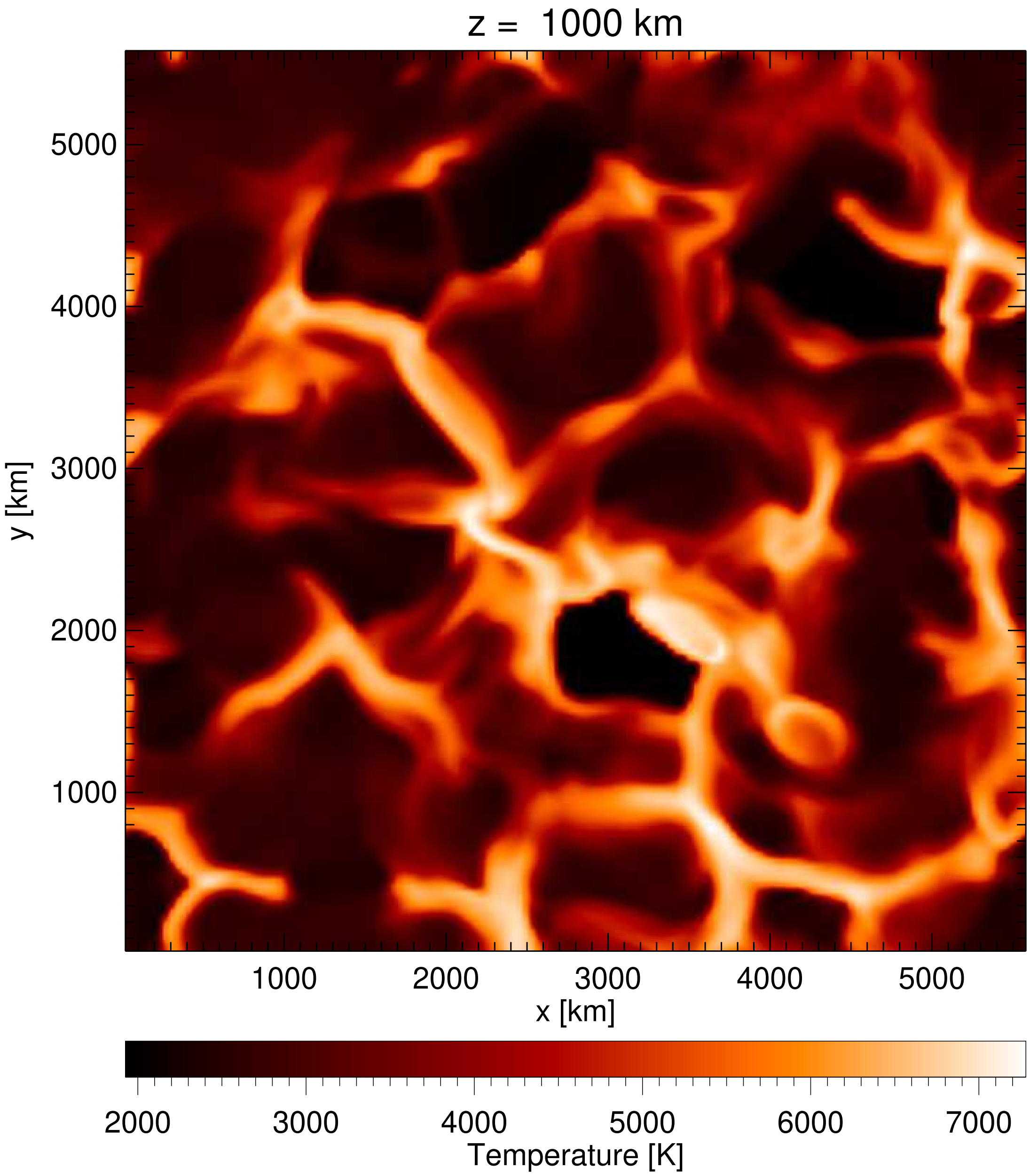

Fig.2: Snapshot of the temperature in a horizontal slice from our preliminary 3-D model at a height of 1000 km (middle chromosphere): Hot wave fronts and cool regions.

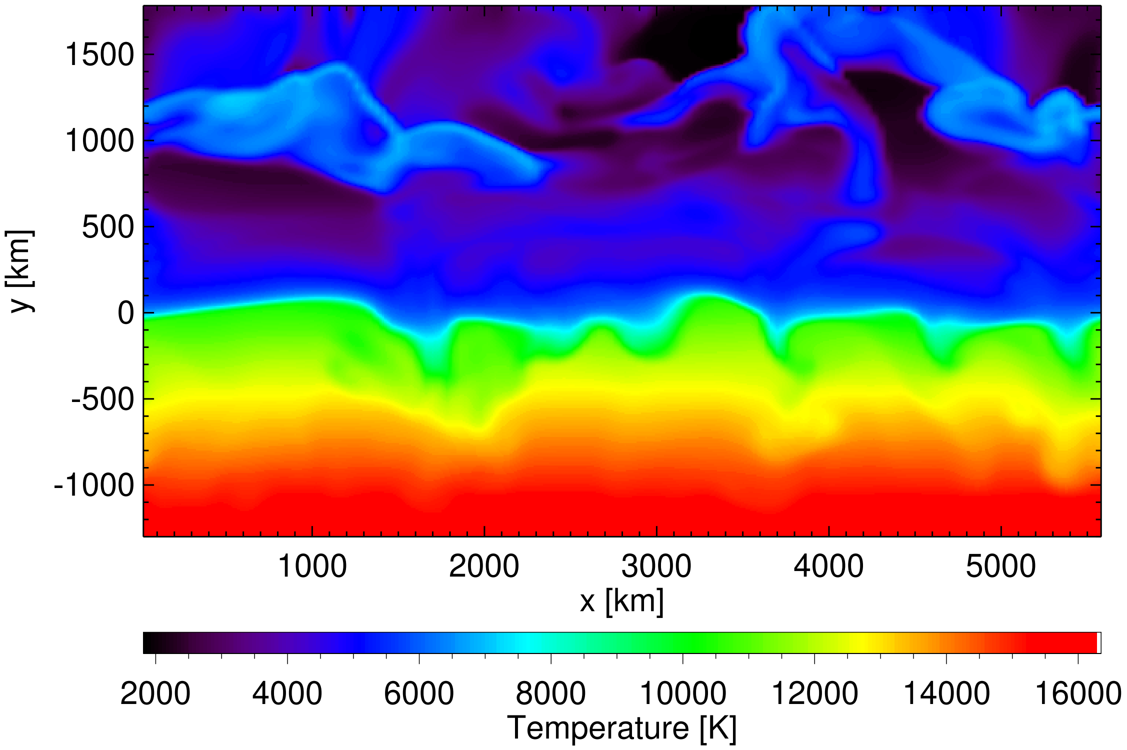

Fig.3: Snapshot of the temperature in a vertical slice from our preliminary 3-D model: Top of the convection zone, photosphere and low/middle chromosphere with propagating shock waves.

A dynamic 3-D model of the solar chromosphere

At the top of the convection zone acoustic waves are excited e.g. by the merging of downdrafts (Skartlien et al., 2000). The wave fronts then propagate upward, gain speed and finally become shock waves (Fig.3). On their way through the chromosphere these shock waves collide and form even more bizarre structures with small-scale brightnings, a **network of hot matter**, representing the travelling wave fronts, and enclosed **cool regions** (Fig.2). These structures are present in the whole low/middle chromosphere of our models at all times and evolve on rather short time-scales.

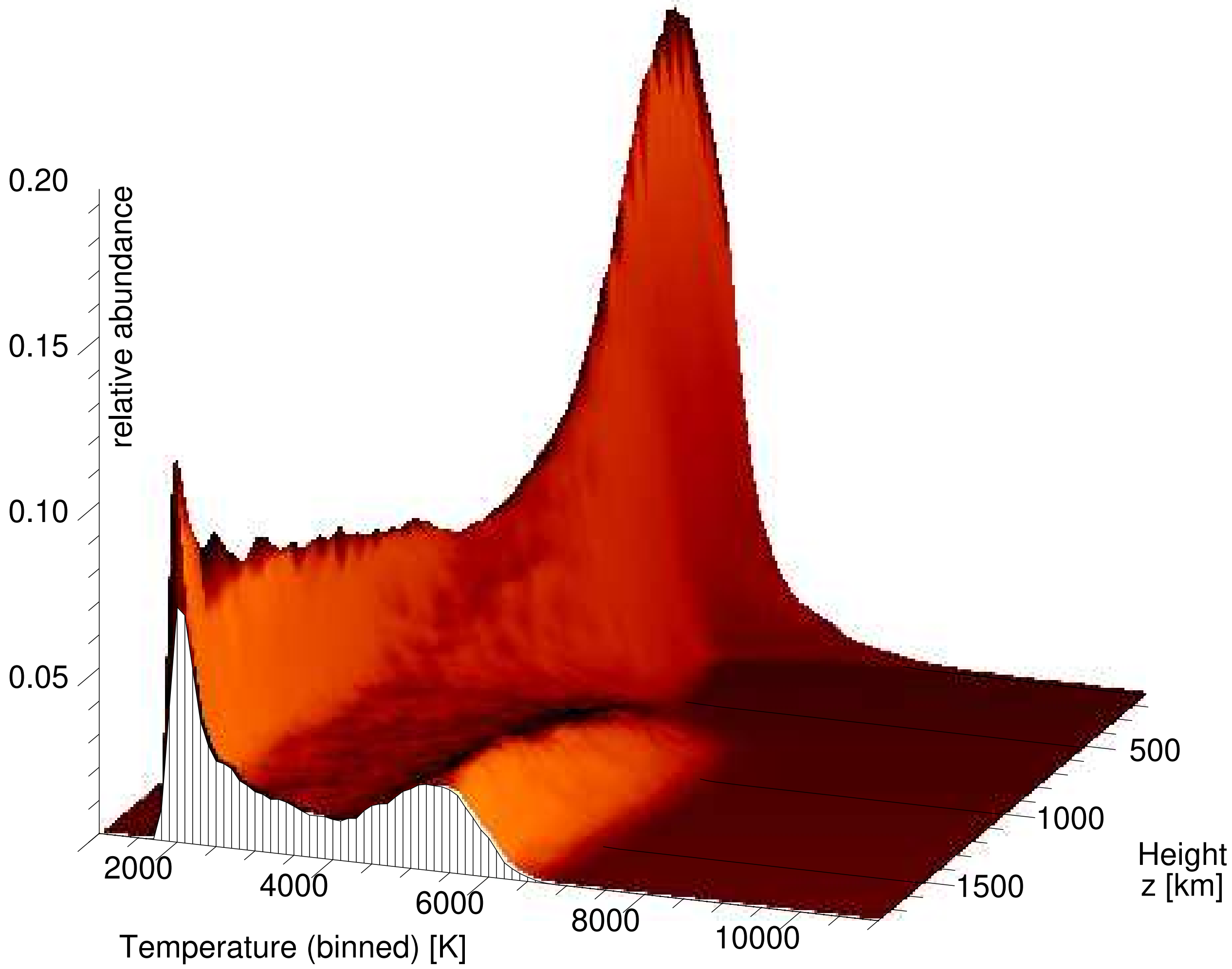

Fig.4: Height-dependent temperature histogram: All temperature values of a 3-D model are sorted into temperature bins of $\Delta T = 100\,\mathrm{K}$ (indicated by vertical lines) for each height independently. The vertical axis denotes the relative abundance of grid cells within a temperature bin with respect to all cells at that height.
Note the **thermal bifurcation in the chromosphere**.

Thermal bifurcation: A hot and cold chromosphere

In Fig.4 the temperature distribution is shown as a function of height. In the photosphere the temperature is distributed close to a mean value with only moderate deviations, whereas, in the chromosphere, the distribution splits up into low and high temperatures with an intermediate range. This **thermal bifurcation**, caused by the co-existence of a cool background and hot shock waves, is a prominent feature in our simulations.

Cool regions and CO molecules

A cool region is only a temporary phenomenon which lasts until the next hot wave front arrives. The temperature in a cool region remains below a temperature of e.g. 3700 K for $50 - 70$ sec in average. But since the passage of a shock wave is a rather short event, the average chromosphere stays half of the total time below 3700 K.
During these relatively short **cool periods** the physical conditions may allow the formation of molecules like carbon monoxide but yet it is not clear how the temporal behaviour affects the formation, existence and dissociation of **CO molecules** and if the resulting abundance is sufficient to explain the observations.

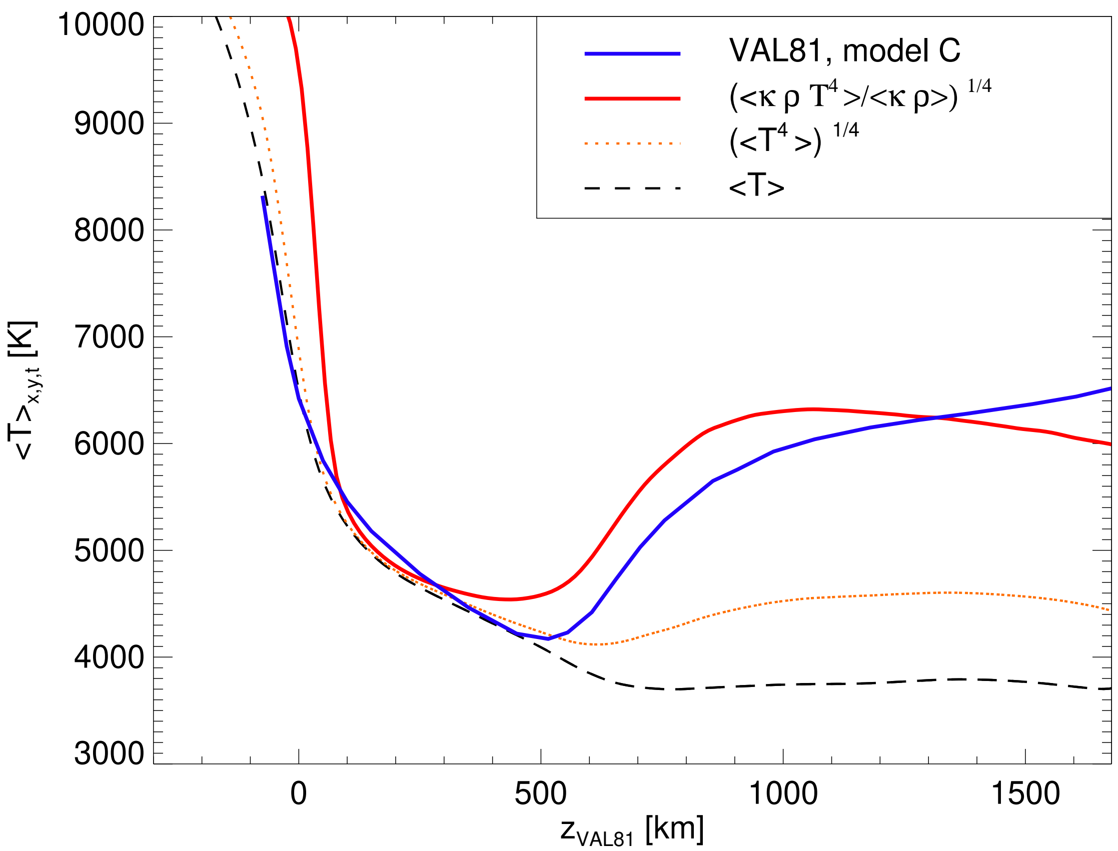

Fig.5: Time-averaged temperature stratifications: The simple arithmetic average (black) and the average emissivity temperature (red) for our preliminary 3-D model, and for comparison model C by Vernazza et al. (1981) (blue).

Temperature stratification

Despite the hot shock waves the temporally and horizontally averaged temperature (simple arithmetic average) decreases with height (black line in Fig.5) and does not show a notable temperature minimum nor a significant temperature increase in the chromosphere like it is the case in the semi-empirical models by Vernazza et al. (1981, hereafter VAL81) and by Fontenla et al. (1993). This mismatch is partly caused by the thermal bifurcation in our models and the applied averaging method. Since the temperature in the VAL C model is derived from observed intensities, a more appropriate averaging method should take into account the different emissivity of the cold and the hot regions in our models. Thus, we calculated an **"average emissivity temperature"**:

$$T_{\rm em}(t,z) = \left(\frac{\langle\, \kappa\, \rho\, T^4\, \rangle_{x,y}}{\langle\, \kappa\, \rho\, \rangle_{x,y}} \right)^{1/4}$$

(ρ: density, κ: opacity, $\langle\,\rangle_{x,y}$: horizontal average)

The average emissivity temperature is shown as red line in Fig.5 which is much more similar to VAL81 C - with regard to the presence of a temperature minimum and the average temperature reached in the middle chromosphere.

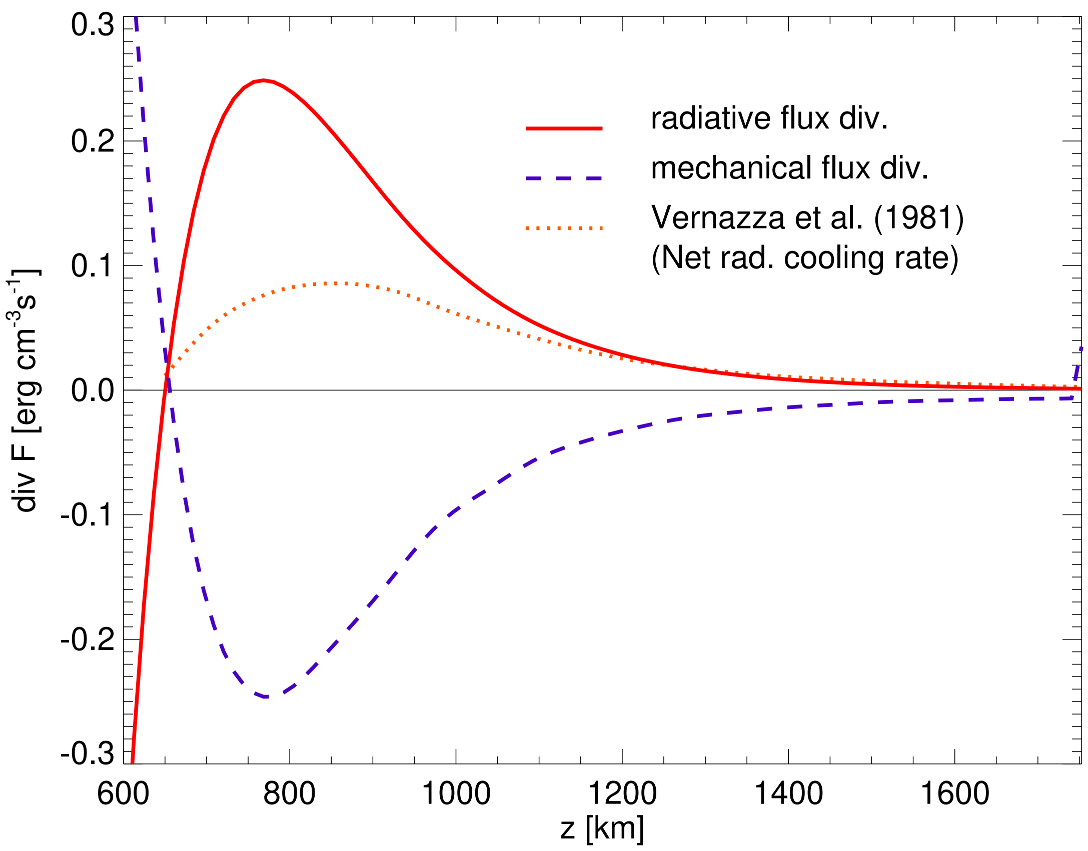

Fig.6: Horizontally and temporally averaged divergence of the radiative (red) and the mechanical energy flux (blue) for our preliminary 3-D model, and the net radiative cooling rate by Vernazza et al. (1981) (orange).

Radiative and mechanical energy flux

Due to the fact that COBOLD is a conservative code the total energy flux is constant. It can be divided into a mechanical and radiative energy flux:

$$F_{\text{total}} = F_{\text{mech}} - F_{\text{rad}}$$

In the chromosphere the energy transport by radiation clearly dominates, leading to a mechanical flux small compared to the radiative one, both almost constant with height. Nevertheless, there are small contributions (source and sink terms) which can be made visible via the flux divergence:

$$\text{div}\vec{F} = \vec{\nabla} \bullet \vec{F} = \frac{\partial F_x}{\partial x} + \frac{\partial F_y}{\partial y} + \frac{\partial F_z}{\partial z}$$

It can be seen from the horizontally and temporally averaged flux divergence (Fig.6) that mechanical flux is converted into radiative flux with a maximum at $z \sim 750$ km. We interpret this as **dissipation of acoustic waves** and emission of radiation. The net radiative cooling rate given by Vernazza et al. (1981) is at least qualitatively similar to the radiative flux divergence in our preliminary 3-D model. In both, the decrease above the local maximum is proportional to the density as predicted by theory.

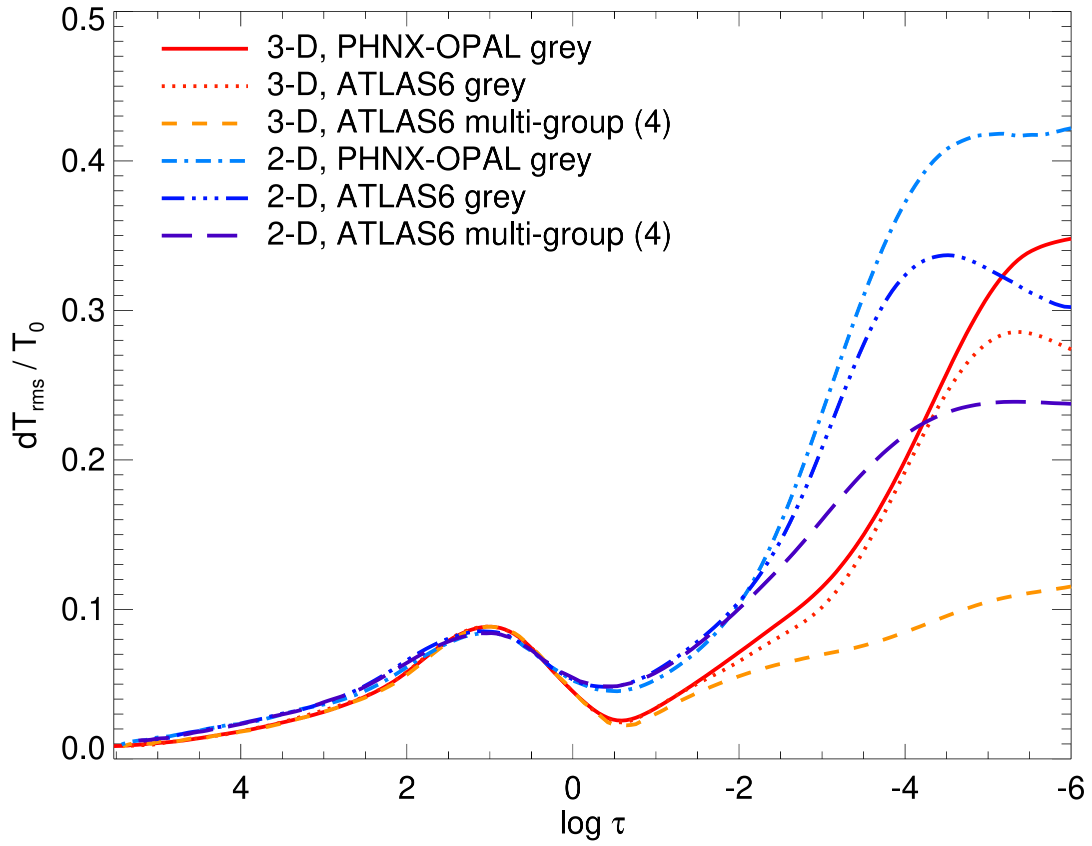

Fig.7: Temperature fluctuation $dT_{\rm rms}/T_0$ for different models on a optical depth scale to illustrate differences caused by the following assumptions: 2-D/3-D, ATLAS6/PHOENIX-OPAL opacities, and grey/multi-group radiation transport.

Dependence on model assumptions

To examine the influence of particular model assumptions on the results presented above, we compare different 2-D and 3-D models. In Fig.7 we show the average temperature fluctuation

$$\frac{dT_{\rm rms}}{T_0} = \frac{\sqrt{< (T- < T >_{x,y,t})^2 >_{x,y,t}}}{< T >_{x,y,t}}$$

for six models to illustrate the influence of 2-D/3-D, the opacity table, and grey/multi-group radiation transport. The dimension (2-D/3-D) leads already at the bottom of the photosphere to differences in $dT_{\rm rms}/T_0$, whereas the influence of opacity and radiation transport becomes significant at smaller optical depths ($>$ high photosphere).

Conclusions

Although still some details need to be optimized for chromospheric conditions (especially the radiative transfer), the first preliminary 3-D simulations already yield interesting results, such as the dissipation of more mechanical energy flux in the low chromosphere than derived from observations. Based on these preliminary results, no additional heating by magnetic effects seems to be necessary for the low and middle chromosphere of our models (Quiet Sun).

Perhaps more important and less susceptible to particular model assumptions is the complex structure of our model chromosphere which is caused by the interaction of shock waves. The resulting thermal bifurcation, i.e. the co-existence of cold and hot regions, could even allow to combine the ”hot” chromosphere models (like VAL81 C) with temperatures high enough to produce chromospheric emission lines and the ”mostly cold” models (like Carlsson & Stein, 1995) with regions cold enough for molecular features (e.g. CO) at the same time and thus might be very important for the interpretation of observations.

Literature

Carlsson, M., Stein, R.F., 1995, ApJ 440, L29
Fontenla, J.M., Avrett, E.H., Loeser, R., 1993, ApJ 406, 319
Hauschildt, P.H., Baron, E., Allard, F. 1997, ApJ 483, 390
Iglesias, C.A., Rogers, F.J., Wilson, B.G. 1992, ApJ 397, 717
Kurucz, R. L., 1970, SAO Special Report, Cambridge
Skartlien, R., Nordlund, Å., Stein, R.F., 2000, ApJ 541, 468
Vernazza, J.E., Avrett, E.H., Loeser, R., 1981, ApJS 45, 635